

Faraday Patterns in Bose-Einstein Condensates

Tatjana S. Wiese

October 30, 2006

Abstract

Parametric excitation of Bose-Einstein condensates (BECs) has been shown numerically to create similar patterns as those produced when a liquid is vibrated up and down sinusoidally. In this project, we reproduce the results of single-frequency forcing in BECs and conduct a preliminary investigation of double-frequency forcing. We analyze the stability of the spatially homogeneous, temporally periodic solution of the Gross-Pitaevskii (GP) equation, which describes the macroscopic dynamics of BECs, by perturbing it and investigating the linear Mathieu equation governing the dynamics of the perturbation numerically and analytically. Patterns in different stability regimes can be visualized by numerically integrating the GP equation.

The manifestation of similar patterns in disparate systems suggests that there is a universality in appropriate coarse-grained descriptions of their underlying dynamics. The Faraday experiment provides one important pattern-forming system that serves as an example of such ubiquity. By forcing waves on the surface of a fluid parametrically one can produce ‘Faraday patterns’ of various forms [1]. If two different sinusoidal forcings are applied to the same fluid, patterns can appear on different scales—these are called superlattice patterns [3], [4]. It has been shown numerically that parametric excitation of Bose-Einstein condensates yields Faraday-like patterns, exemplifying the universality discussed above. This paper describes the duplication of known results about the Faraday patterns formed in Bose-Einstein condensates with one sinusoidal forcing term [5], and a preliminary investigation of the patterns formed when two sinusoidal forcing terms are present.

1 Introduction

The Faraday experiment consists of forcing a fluid sinusoidally up and down. The container of the fluid is placed on a machine that induces vibrations normal to the surface, and light shining through the fluid is recorded by a camera. If the amplitude of the driving acceleration is large enough to exceed the dissipation

from viscosity, patterns known as ‘Faraday patterns’, appear. Depending on the oscillation frequency and the viscosity of the fluid, different patterns are produced—including stripes at high viscosity, squares at lower viscosity and high frequency, and more complex shapes at low viscosity and low frequency [1]. More recent technologies have allowed scientists more control of experimental parameters, which has resulted in observation of more intricate patterns [2]. If one includes the effect of damping, there are additional dissipative terms that ensure that the system is heading towards a ground state, inhibiting instability for certain parameter values [3]. If two forcings, which may differ in amplitude or driving frequency and may also be phase-shifted from each other, are applied, so-called ‘superlattice patterns’, which are patterns on different scales, can arise [4], [3]. An example of a superlattice pattern is shown in Figure 1.

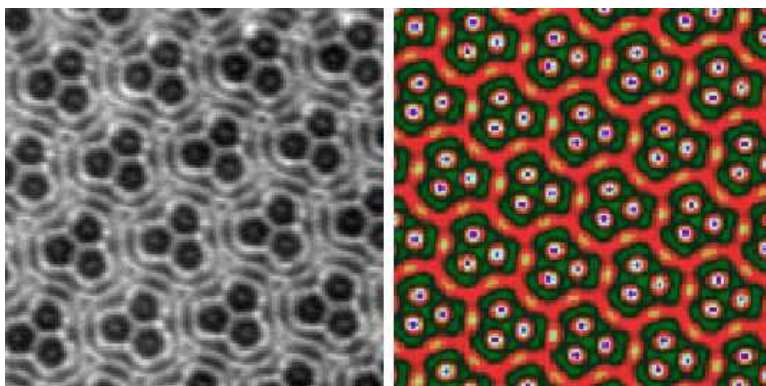


Figure 1: Superlattice pattern produced by a double-frequency forcing of 6:7. The image on the left was experimentally observed in [6] and the figure on the right was computed numerically in [7]. Combined figure courtesy of Hermann Riecke.

Similar Faraday patterns have been found in numerical studies of parametrically forced Bose-Einstein Condensates (BECs) [5]. A BEC is a state of matter that occurs when a dilute gas of bosons is cooled to temperatures near absolute zero so that the de Broglie wavelength is on the order of the interatomic separation. At this point, most of the atoms are in the same quantum mechanical state and the gas has become a coherent ‘matter wave’ [8]. The analogue of forcing the surface of the fluid up and down in the Faraday experiment is the periodic modulation of the interatomic s -wave scattering length, a variable that describes the range of the interatomic forces, of the condensate [8], [5]. At certain forcing frequencies, Faraday patterns appear in the atomic density of the BEC in physical space. To investigate these patterns, it is important to understand the dynamics of the Gross-Pitaevskii (GP) equation, which governs the macroscopic (mean-field) dynamics of BECs.

2 The Gross-Pitaevskii Equation

The mean-field dynamics of Bose-Einstein condensates are described using the GP equation [9], a nonlinear partial differential equation. To study Faraday patterns, its nonlinearity coefficient is modulated in time so that the GP equation is written [5]

$$i\frac{\partial\psi}{\partial t} = [-\nabla^2 + V_{trap}(\mathbf{r}) + c(t)|\psi|^2]\psi, \quad (1)$$

where ∇^2 is the Laplacian, $\psi(\mathbf{r}, t)$ is the BEC wavefunction and $V_{trap}(\mathbf{r})$ is an external potential. The nonlinearity coefficient $c(t) = 1 + 2\alpha \cos(2\omega t)$, where α is the amplitude and ω determines the frequency of modulation, was used in [5] to study single-frequency forcing. To study double-frequency forcing, one lets $c(t) = 1 + 2[\alpha_1 \cos(2\omega_1 t) + \alpha_2 \cos(2\omega_2 t)]$ [5].

To study the single-frequency, undamped spatially homogeneous GP equation, we assume the trapping potential is zero and consider solutions of the form

$$\psi(\mathbf{r}, t) = \psi_{hom}(t) \equiv e^{-i(\alpha/\omega) \sin(2\omega t)}. \quad (2)$$

To examine the stability of such solutions, we perturb this spatially homogeneous wavefunction and consider $\psi(\mathbf{r}, t) = \psi_{hom}(t)[1 + \epsilon w(t) \cos(\mathbf{k} \cdot \mathbf{r})]$, where $w(t) = u(t) + iv(t)$ is an unknown function of time, \mathbf{k} is the wavevector of the perturbation, and \mathbf{r} is a position vector. From this, we derive (see section 2) a linear Mathieu equation

$$\frac{d^2u}{dt^2} + [\Omega^2(k) + 4k^2\alpha \cos(2\omega t)]u = 0, \quad (3)$$

where $\Omega = k\sqrt{k^2 + 2}$ describes the dispersion of the perturbation if no driving is present, and k is the magnitude of the wavevector of perturbation \mathbf{k} . This equation is much easier to investigate than the GP equation; one can vary parameters and thereby study the stability of the homogeneous wavefunction indirectly [5].

To incorporate damping, the GP equation is written

$$i\frac{\partial\psi}{\partial t} = (1 - i\gamma)(-\nabla^2 - \mu + |\psi|^2)\psi + 2\alpha \cos(2\omega t)|\psi|^2\psi, \quad (4)$$

where γ is the damping coefficient, and μ , the chemical potential, is set to 1. In this case, an analogous derivation yields a damped Mathieu equation

$$\frac{d^2u}{dt^2} + 2\gamma(1 + k^2)\frac{du}{dt} + [(1 + \gamma^2)\Omega^2(k) + 4k^2\alpha \cos(2\omega t)]u = 0. \quad (5)$$

In considering the case of double-frequency forcing, we arrive at the most general form of the GP equation investigated in this paper:

$$i\frac{\partial\psi}{\partial t} = (1 - i\gamma)(-\nabla^2 - \mu + |\psi|^2)\psi + 2[\alpha_1 \cos(2\omega_1 t) + \alpha_2 \cos(2\omega_2 t)]|\psi|^2\psi, \quad (6)$$

where the two trigonometric terms arise from the parametric vibrations applied to the system. The parameters α_1 and α_2 are the forcing amplitudes and ω_1 and ω_2 are the forcing frequencies [5]. In this case, the Mathieu equation is

$$\frac{d^2 u}{dt^2} + 2\gamma(1 + k^2) \frac{du}{dt} + \{(1 + \gamma^2)\Omega^2(k) + 4k^2[\alpha_1 \cos(2\omega_1 t) + \alpha_2 \cos(2\omega_2 t)]\}u = 0. \quad (7)$$

3 Derivation of the damped Mathieu equation from damped GP equation

The perturbations of the homogeneous solution of the GP equation satisfy the Mathieu equation, for which it is easier to analyze the stability of solutions for different parameter values. We take ψ to be the spatially homogeneous, temporally periodic solution, equation (2), of the GP equation, times a small term of spatial perturbation $1 + \epsilon w(t) \cos(\mathbf{k} \cdot \mathbf{r})$, yielding $\psi = \exp(-i(\alpha/\omega) \sin(2\omega t))(1 + \epsilon w(t) \cos(\mathbf{k} \cdot \mathbf{r}))$. To investigate the damped case with a forcing term $c(t)$, we write equation (4), in which case $c(t) = 1 + 2\alpha \cos(2\omega t)$, as

$$i \frac{\partial \psi}{\partial t} = -\nabla^2 \psi - \psi + i\gamma \nabla^2 \psi + i\gamma \psi - i\gamma |\psi|^2 \psi + c(t) |\psi|^2 \psi. \quad (8)$$

Now we plug ψ into this GP equation. To linearize the GP equation, we must expand the resulting function of ϵ in a Taylor series in ϵ , considering terms up to first order. To do so, we collect terms on one side of the GP equation, to make the other side equal to zero. The zeroth-order term of the Taylor expansion is a consistency condition that cancels out. We set the first-order term, which will ultimately give the linear Mathieu equation, to zero to obtain:

$$\begin{aligned} \psi_{hom} \cos(\mathbf{k} \cdot \mathbf{r}) & \left(-(u(t) + iv(t))k^2 + 2\alpha \cos(2\omega t)(u(t) + iv(t)) + i \frac{du}{dt} \right) \\ & - \frac{dv}{dt} + i\gamma(u(t) + iv(t))k^2 + (u + iv) + 2i\gamma u - c(t)(u + iv) - 2c(t)u = 0 \end{aligned} \quad (9)$$

Because this expression is complex, we set the real and imaginary parts to zero separately, obtaining expressions for $\frac{du}{dt}$ and $\frac{dv}{dt}$:

$$\frac{du}{dt} = -v(t)(-k^2 + 2\alpha \cos(2\omega t) + 1 - c(t)) - u(t)(\gamma k^2 + 2\gamma) \quad (10)$$

$$\frac{dv}{dt} = u(t)(-k^2 + 2\alpha \cos(2\omega t) + 1 - 3c(t)) + v(t)(-\gamma k^2) \quad (11)$$

We differentiate equation (10):

$$\frac{d^2 u}{dt^2} = \frac{dv}{dt} (k^2 - 2\alpha \cos(2\omega t) - 1 + c(t)) + v(t) \left(4\alpha \omega \sin(2\omega t) + \frac{dc}{dt} \right) - \frac{du}{dt} (\gamma k^2 + 2\gamma), \quad (12)$$

and write this equation in terms of u and $\frac{du}{dt}$, using equations (10) and (11). This yields

$$\begin{aligned} \frac{d^2u}{dt^2} = & u(t)[-k^4 + 4k^2\alpha \cos(2\omega t) + 2k^2 - 4k^2c(t) \\ & - 4\alpha \cos(2\omega t) + 8c(t)\alpha \cos(2\omega t) + 4c(t) - 4\alpha^2 \cos^2(2\omega(t)) - 1 - 3c(t)^2 \\ & - \gamma k^2(\gamma k^2 + 2\gamma) - \frac{(\gamma k^2 + 2\gamma)(4\alpha\omega \sin(2\omega t) + \frac{dc}{dt})}{-k^2 + 2\alpha \cos(2\omega t) + 1 - c(t)}] \\ & - \frac{du}{dt} \left(2\gamma k^2 + 2\gamma + \frac{4\alpha\omega \sin(2\omega t) + \frac{dc}{dt}}{-k^2 + 2\alpha \cos(2\omega t) + 1 - c(t)} \right). \end{aligned} \quad (13)$$

Recall that for single-frequency forcing, we let $c(t) = 1 + 2\alpha \cos(2\omega t)$. Equation (13) then becomes

$$\frac{d^2u}{dt^2} + 2\gamma(1 + k^2)\frac{du}{dt} + [(1 + \gamma^2)\Omega^2(k) + 4k^2\alpha \cos(2\omega t)]u = 0, \quad (14)$$

which is the damped linear Mathieu equation. For double-frequency forcing, we would instead substitute $c(t)$ with two trigonometric terms.

4 Stability Analysis

The dynamics of the wavefunction depend on the wavenumber k and on the forcing amplitude α . Some values make equation (14) stable (all solutions are bounded), some make it unstable (there exists at least one unbounded solution), and some yield solutions on the boundary of stable and unstable pairs of parameter values [10]. This boundary consists of a set of one-dimensional transition curves in the k - α plane that separates stable regions from unstable regions. This means that if we plot the wavenumber k versus the amplitude α as ordered pairs (k, α) on a coordinate plane, the unstable pairs and the stable pairs will be separated by curves.

Methods for analyzing the stability of the Mathieu equation for different values of parameters include multiple-scale expansions, with which one obtains points where transition curves intersect the k -axis (and can express the transition curves to the first order in k), and the method of harmonic balance, with which one can obtain more precise approximations to the transition curves [10]. In this work, we focus primarily on the latter.

4.1 Harmonic balance

This derivation is described mostly in Rand's notes on nonlinear vibrations [10], and unless otherwise indicated, the information in this section should be assumed to be from that source. For simplicity, we write the Mathieu equation as:

$$\frac{d^2u}{dt^2} + [\delta + \epsilon \cos(2\omega t)]u = 0, \quad (15)$$

where $\epsilon = 4k^2\alpha$ and $\delta = k^2(k^2 + 2)$. This means the transition curves will now be in the δ - ϵ plane. This rescaled Mathieu equation contains a periodic term of period π/ω . From Floquet theory, we obtain the result that on the transition curves there exist periodic solutions of period π/ω and $2\pi/\omega$. Therefore, it is possible to represent $u(t)$ as a Fourier series [10], [11], [12]:

$$u(t) = \sum_{n=0}^{\infty} a_n \cos\left(\frac{nt}{2}\right) + b_n \sin\left(\frac{nt}{2}\right), \quad (16)$$

where we have let $\omega = 1/2$. Floquet theory applies to double-frequency forcing if ω_1/ω_2 is rational, for then the sum of the two trigonometric terms is still periodic. If the ratio of ω_1 and ω_2 is irrational, one cannot apply Floquet theory because the Mathieu equation would not have a periodic term [13].

Inserting the Fourier series (16) into the Mathieu equation and collecting linearly independent terms, one obtains an infinite set of homogeneous linear equations, so the determinant of the infinite matrix of their coefficients must be zero for the Mathieu equation to be satisfied. The determinant can be truncated as long as ϵ is small, and the power of ϵ at which the truncation occurs determines the accuracy of the expressions for the transition curves [10]. I have calculated several truncated determinants in the undamped single-frequency case and some examples in the undamped double-frequency case.

Rescaling equation (7), with $\delta = k^2(k^2 + 2)$ and $\epsilon = 4k^2$ and letting $\gamma = 0$, we calculate an example for the double-frequency case. The Mathieu equation is written

$$\frac{d^2u}{dt^2} + \{\delta + \epsilon[\alpha_1 \cos(\omega_1 t) + \alpha_2 \cos(\omega_2 t)]\}u = 0. \quad (17)$$

Consider $(\omega_1, \omega_2) = (1, 2)$. From equation (7), we obtain the second derivative

$$\frac{d^2u}{dt^2} = - \sum_{n=0}^{\infty} \frac{n^2}{4} \left[a_n \cos\left(\frac{nt}{2}\right) + b_n \sin\left(\frac{nt}{2}\right) \right]. \quad (18)$$

We then insert equations (16) and (18) into equation (17) to obtain an algebraic equation that must be satisfied [11]:

$$\sum_{n=0}^{\infty} \left[a_n \cos\left(\frac{nt}{2}\right) + b_n \sin\left(\frac{nt}{2}\right) \right] \left[\delta + \epsilon\alpha_1 \cos(t) + \epsilon\alpha_2 \cos(2t) - \frac{n^2}{4} \right] = 0. \quad (19)$$

Now we calculate the harmonic equations to the degree desired, and truncate at an n of our choice. The choice $n = 8$ is convenient because the irregularities that occur for the first few n disappear within the first three rows in the even and odd cases, and this way we can display at least two regular rows in each determinant (showing four n). Now combine terms with the same period; this is where the method gets its name [11]. Because terms with even n and odd n , as well as sines and cosines, are independent of each other, we obtain separate

determinants for each:

$$\begin{aligned}
a_{even} : & \begin{vmatrix} \delta & \frac{\epsilon}{2}\alpha_1 & \frac{\epsilon}{2}\alpha_2 & 0 & 0 & 0 & 0 & 0 \\ \epsilon\alpha_1 & \delta - 1 + \frac{\epsilon}{2}\alpha_2 & \frac{\epsilon}{2}\alpha_1 & \frac{\epsilon}{2}\alpha_2 & 0 & 0 & 0 & 0 \\ \epsilon\alpha_2 & \frac{\epsilon}{2}\alpha_1 & \delta - 4 & \frac{\epsilon}{2}\alpha_1 & \frac{\epsilon}{2}\alpha_2 & 0 & 0 & 0 \\ 0 & \frac{\epsilon}{2}\alpha_2 & \frac{\epsilon}{2}\alpha_1 & \delta - 9 & \frac{\epsilon}{2}\alpha_1 & \frac{\epsilon}{2}\alpha_2 & 0 & 0 \\ 0 & 0 & \frac{\epsilon}{2}\alpha_2 & \frac{\epsilon}{2}\alpha_1 & \delta - 16 & \frac{\epsilon}{2}\alpha_1 & \frac{\epsilon}{2}\alpha_2 & 0 \\ 0 & 0 & 0 & \frac{\epsilon}{2}\alpha_2 & \frac{\epsilon}{2}\alpha_1 & \delta - 25 & \frac{\epsilon}{2}\alpha_1 & \frac{\epsilon}{2}\alpha_2 \\ 0 & 0 & 0 & 0 & \frac{\epsilon}{2}\alpha_2 & \frac{\epsilon}{2}\alpha_1 & \delta - 36 & \frac{\epsilon}{2}\alpha_1 \\ 0 & 0 & 0 & 0 & 0 & \frac{\epsilon}{2}\alpha_2 & \frac{\epsilon}{2}\alpha_1 & \delta - 49 \end{vmatrix} = 0 \\
a_{odd} : & \begin{vmatrix} \delta - \frac{1}{4} + \frac{\epsilon}{2}\alpha_1 & \frac{\epsilon}{2}(\alpha_1 + \alpha_2) & \frac{\epsilon}{2}\alpha_2 & 0 & 0 & 0 & 0 & 0 \\ \frac{\epsilon}{2}(\alpha_1 + \alpha_2) & \delta - \frac{9}{4} & \frac{\epsilon}{2}\alpha_1 & \frac{\epsilon}{2}\alpha_2 & 0 & 0 & 0 & 0 \\ \frac{\epsilon}{2}\alpha_2 & \frac{\epsilon}{2}\alpha_1 & \delta - \frac{25}{4} & \frac{\epsilon}{2}\alpha_1 & \frac{\epsilon}{2}\alpha_2 & 0 & 0 & 0 \\ 0 & \frac{\epsilon}{2}\alpha_2 & \frac{\epsilon}{2}\alpha_1 & \delta - \frac{49}{4} & \frac{\epsilon}{2}\alpha_1 & \frac{\epsilon}{2}\alpha_2 & 0 & 0 \\ 0 & 0 & \frac{\epsilon}{2}\alpha_2 & \frac{\epsilon}{2}\alpha_1 & \delta - \frac{81}{4} & \frac{\epsilon}{2}\alpha_1 & \frac{\epsilon}{2}\alpha_2 & 0 \\ 0 & 0 & 0 & \frac{\epsilon}{2}\alpha_2 & \frac{\epsilon}{2}\alpha_1 & \delta - \frac{121}{4} & \frac{\epsilon}{2}\alpha_1 & \frac{\epsilon}{2}\alpha_2 \\ 0 & 0 & 0 & 0 & \frac{\epsilon}{2}\alpha_2 & \frac{\epsilon}{2}\alpha_1 & \delta - \frac{169}{4} & \frac{\epsilon}{2}\alpha_1 \\ 0 & 0 & 0 & 0 & 0 & \frac{\epsilon}{2}\alpha_2 & \frac{\epsilon}{2}\alpha_1 & \delta - \frac{225}{4} \end{vmatrix} = 0 \\
b_{even} : & \begin{vmatrix} \delta - 1 - \frac{\epsilon}{2}\alpha_2 & \frac{\epsilon}{2}\alpha_1 & \frac{\epsilon}{2}\alpha_2 & 0 & 0 & 0 & 0 & 0 \\ \frac{\epsilon}{2}\alpha_1 & \delta - 4 & \frac{\epsilon}{2}\alpha_1 & \frac{\epsilon}{2}\alpha_2 & 0 & 0 & 0 & 0 \\ \frac{\epsilon}{2}\alpha_2 & \frac{\epsilon}{2}\alpha_1 & \delta - 9 & \frac{\epsilon}{2}\alpha_1 & \frac{\epsilon}{2}\alpha_2 & 0 & 0 & 0 \\ 0 & \frac{\epsilon}{2}\alpha_2 & \frac{\epsilon}{2}\alpha_1 & \delta - 16 & \frac{\epsilon}{2}\alpha_1 & \frac{\epsilon}{2}\alpha_2 & 0 & 0 \\ 0 & 0 & \frac{\epsilon}{2}\alpha_2 & \frac{\epsilon}{2}\alpha_1 & \delta - 25 & \frac{\epsilon}{2}\alpha_1 & \frac{\epsilon}{2}\alpha_2 & 0 \\ 0 & 0 & 0 & \frac{\epsilon}{2}\alpha_2 & \frac{\epsilon}{2}\alpha_1 & \delta - 36 & \frac{\epsilon}{2}\alpha_1 & \frac{\epsilon}{2}\alpha_2 \\ 0 & 0 & 0 & 0 & \frac{\epsilon}{2}\alpha_2 & \frac{\epsilon}{2}\alpha_1 & \delta - 49 & \frac{\epsilon}{2}\alpha_1 \\ 0 & 0 & 0 & 0 & 0 & \frac{\epsilon}{2}\alpha_2 & \frac{\epsilon}{2}\alpha_1 & \delta - 64 \end{vmatrix} = 0 \\
b_{odd} : & \begin{vmatrix} \delta - \frac{1}{4} - \frac{\epsilon}{2}\alpha_1 & \frac{\epsilon}{2}(\alpha_1 - \alpha_2) & \frac{\epsilon}{2}\alpha_2 & 0 & 0 & 0 & 0 & 0 \\ \frac{\epsilon}{2}(\alpha_1 - \alpha_2) & \delta - \frac{9}{4} & \frac{\epsilon}{2}\alpha_1 & \frac{\epsilon}{2}\alpha_2 & 0 & 0 & 0 & 0 \\ \frac{\epsilon}{2}\alpha_2 & \frac{\epsilon}{2}\alpha_1 & \delta - \frac{25}{4} & \frac{\epsilon}{2}\alpha_1 & \frac{\epsilon}{2}\alpha_2 & 0 & 0 & 0 \\ 0 & \frac{\epsilon}{2}\alpha_2 & \frac{\epsilon}{2}\alpha_1 & \delta - \frac{49}{4} & \frac{\epsilon}{2}\alpha_1 & \frac{\epsilon}{2}\alpha_2 & 0 & 0 \\ 0 & 0 & \frac{\epsilon}{2}\alpha_2 & \frac{\epsilon}{2}\alpha_1 & \delta - \frac{81}{4} & \frac{\epsilon}{2}\alpha_1 & \frac{\epsilon}{2}\alpha_2 & 0 \\ 0 & 0 & 0 & \frac{\epsilon}{2}\alpha_2 & \frac{\epsilon}{2}\alpha_1 & \delta - \frac{121}{4} & \frac{\epsilon}{2}\alpha_1 & \frac{\epsilon}{2}\alpha_2 \\ 0 & 0 & 0 & 0 & \frac{\epsilon}{2}\alpha_2 & \frac{\epsilon}{2}\alpha_1 & \delta - \frac{169}{4} & \frac{\epsilon}{2}\alpha_1 \\ 0 & 0 & 0 & 0 & 0 & \frac{\epsilon}{2}\alpha_2 & \frac{\epsilon}{2}\alpha_1 & \delta - \frac{225}{4} \end{vmatrix} = 0.
\end{aligned}$$

The columns of each determinant correspond to increasing n (starting at $n = 0$), and the rows correspond to increasing harmonics. Thus, for a_{even} and b_{even} , I kept $n = 0, 2, 4, 6, 8, 10, 12, 14$ and harmonics of $\cos(rt)$, $r = 0, 1, 2, 3, 4, 5, 6, 7$, and for a_{odd} and b_{odd} , I kept $n = 1, 3, 5, 7, 9, 11, 13, 15$ and harmonics of $\cos(rt)$, $r = \frac{1}{2}, \frac{3}{2}, \frac{5}{2}, \frac{7}{2}, \frac{9}{2}, \frac{11}{2}, \frac{13}{2}, \frac{15}{2}$. The aforementioned irregularities, namely the fact that the first few rows of the determinants are not of the form $\left[\frac{\epsilon}{2}\alpha_2, \frac{\epsilon}{2}\alpha_1, \delta - \frac{n^2}{4}, \frac{\epsilon}{2}\alpha_1, \frac{\epsilon}{2}\alpha_2\right]$, arise from special values (such as zero) of the trigonometric functions.

Because each of these determinants equals zero, we obtain a relation between δ and ϵ that will give us approximations to transition curves.

The next step is to express δ as a power series in ϵ to an order of our choice, depending on how many terms we want in the equation for the transition curves. If we set $\epsilon = 0$ in the determinants, we obtain the intersections of the transition curves with the δ -axis. With $\epsilon = 0$, the determinants are the products of the diagonal entries. Hence, the transition curves from a_{even} and b_{even} have

zeroes at $\delta = n^2, n = 0, 1, 2, 3, \dots$ and the transition curves from a_{odd} and b_{odd} would have zeroes at $\delta = \frac{(2n+1)^2}{4}$. Because the successive squares of the even numbers are divisible by four (and are the successive squares of the integers), the intersection of the transition curves with the δ -axis occurs at

$$\delta = \frac{n^2}{4}. \quad (20)$$

Figures 2 and 3 show ‘tongues’ of instability emanating from each intersection. The two curves that form each tongue come from the corresponding a -terms and b -terms. The transition curves take the form

$$\delta = \frac{n^2}{4} + \delta_1\epsilon + \delta_2\epsilon^2 + \dots \quad (21)$$

We determine the coefficients in the power series by substituting into the above determinants. Collecting like terms and plotting in the δ - ϵ plane, we obtain images of the transition curves.

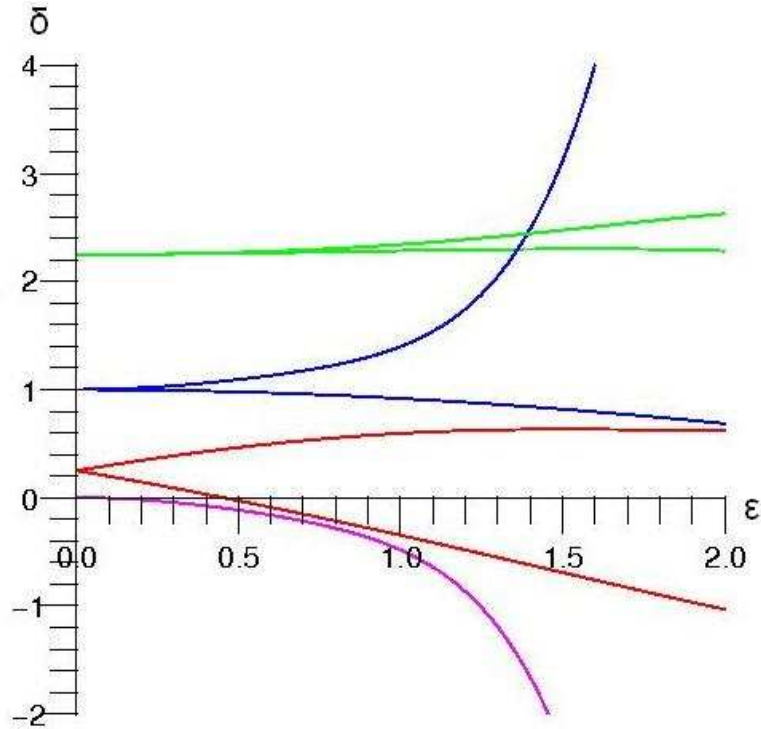


Figure 2: Transition curves for single-frequency forcing, ($n = 0, 1, 2, 3$).

As examples, we display the formulas for the transition curves for $n = 0$. I also computed formulas for the curves at $n = 1, 2, 3$. The equation for the curve emanating from zero in Figure 2 is

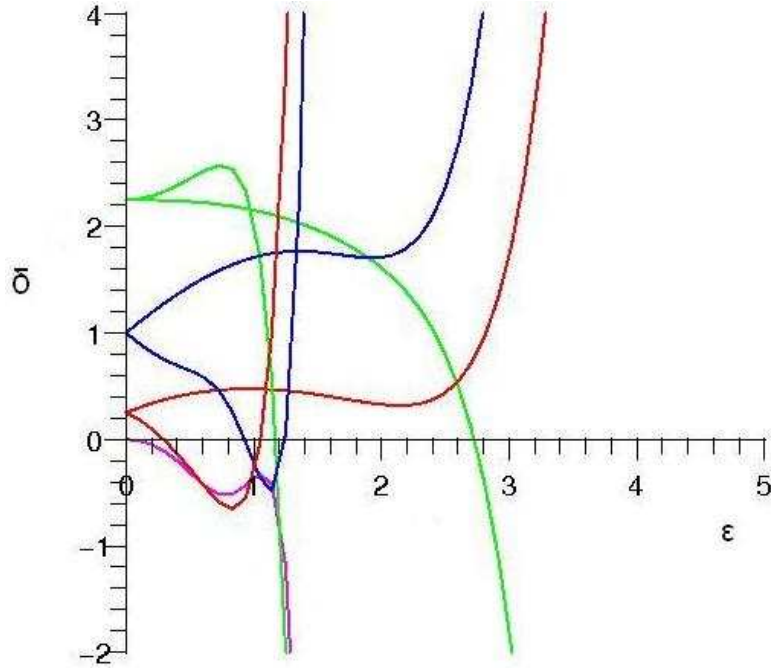


Figure 3: Transition curves for double-frequency forcing for $(\alpha_1, \alpha_2) = (1, 2)$, $(n=0,1,2,3)$.

$$\delta = -\frac{1}{2}\epsilon^2 + \frac{7}{32}\epsilon^4 - \frac{29}{144}\epsilon^6 - \frac{68687}{294912}\epsilon^8 + \dots \quad (22)$$

The equation for the curve emanating from zero in Figure 3 is

$$\begin{aligned} \delta = & -\frac{5}{8}\epsilon^2 - \frac{3}{8}\epsilon^3 + \frac{1535}{18432}\epsilon^4 + \frac{4109}{9216}\epsilon^5 \\ & + \frac{1084207}{3686400}\epsilon^6 - \frac{823171}{2211840}\epsilon^7 - \frac{49864148440471}{59929893273600}\epsilon^8 + \dots \end{aligned} \quad (23)$$

It is important to note that the transition curves are only accurate for small ϵ , so the behavior exhibited in figures 2 and 3 represents the behavior of the solutions of the GP equation less accurately the farther we look to the right.

5 Unresolved Issues

By numerically integrating the GP equation, one can show snapshots of the spatial atom density of the BEC by plotting $|\psi|^2$ in space at particular slices in time [5]. A goal of this project was to duplicate the images (see 4) shown in [5] for single-frequency forcing to become familiar with the split-step method

and to test the validity of code implementing, and then to numerically study the double-frequency case. Unfortunately, I was unable to determine the exact initial conditions used to obtain the images in Figure 4. Nevertheless, I attempted to integrate equation (1) by a split-step routine obtained by modifying a program originally used for calculations in nonlinear optics [14].

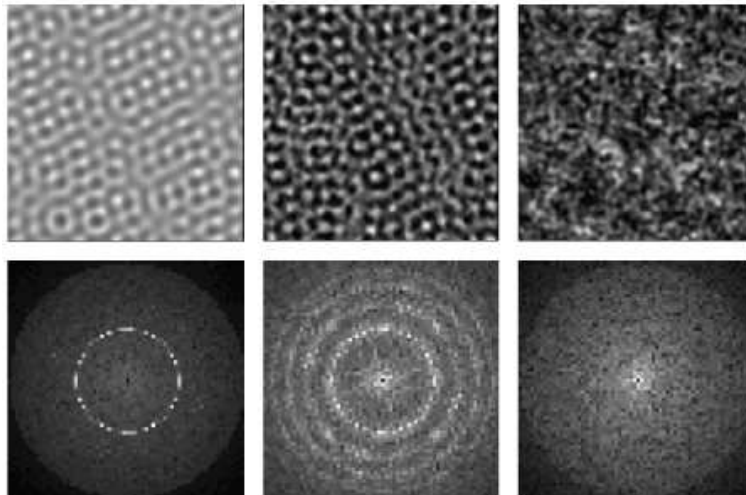


Figure 4: Atom density of parametrically forced BECs at times $t = 100$, $t = 200$, and $t = 300$ (left to right) in physical (top row) and Fourier space (bottom row). In this case, $\alpha = 0.2$ and $\omega = 1.5\pi$. The image was obtained from [5] and is used with permission from Germán de Valcárcel.

I examined several likely initial conditions. The perturbed homogeneous solution $\psi(\mathbf{r}, t) = \psi_{hom}(t)(1+w(t) \cos(\mathbf{k}\cdot\mathbf{r})) = e^{-i(\alpha/\omega)\sin(2\omega t)}(1+w(t) \cos(\mathbf{k}\cdot\mathbf{r}))$ yielded stripes with $w(t)$ constant, and ψ_{hom} multiplied by a small random perturbation yielded patterns but not the desired ones. I also used an initial condition obtained by scanning the image from the paper. The purpose of the latter was to better test the code without the precise knowledge of the initial conditions.

5.1 The Split-Step Method

To numerically simulate the GP equation (1), one can treat its linear and nonlinear parts $\psi_L = i\nabla^2\psi_L$ and $\psi_N = -ic(t)|\psi_N|^2\psi_N$ separately. The former is solved in Fourier space and the latter in real space [15]. If each term is advanced by a small time step Δt successively N times, one obtains an approximate solution ψ at $t = N\Delta t$ [14]. The step Δt must be small for such a superposition to give reasonable results for a nonlinear equation like the GP equation.

The given code was written in physical units, which were unnecessary for our purposes. Also, my time variable was their distance-propagation variable; the

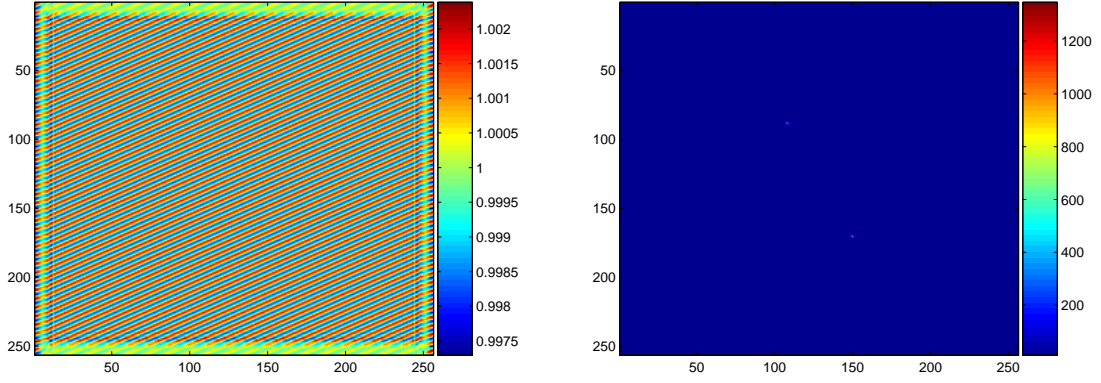


Figure 5: Patterns in physical space (left) and Fourier space (right) in simulation of the GP equation when the initial condition is the perturbed homogeneous solution $\psi(\mathbf{r}, t) = \psi_{hom}(t)(1+w(t) \cos(\mathbf{k}\cdot\mathbf{r})) = e^{-i(\alpha/\omega)\sin(2\omega t)}(1+w(t) \cos(\mathbf{k}\cdot\mathbf{r}))$, created with MATLAB. There is only one vector of perturbation, as can be seen in Fourier space.

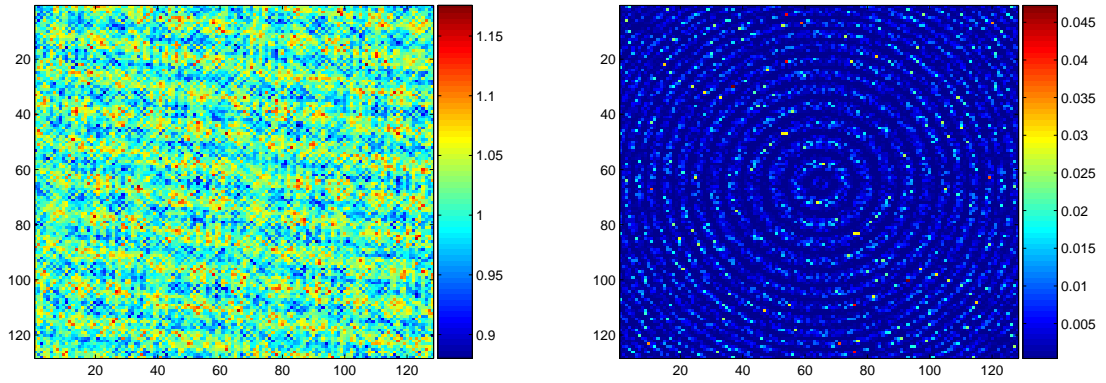


Figure 6: Patterns in physical space (left) and Fourier space (right) when the initial condition is the homogeneous solution times a small random perturbation.

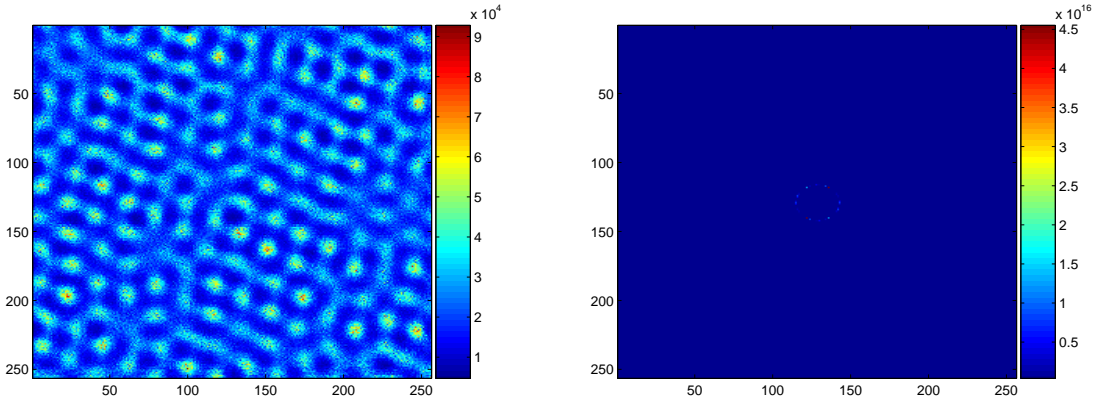


Figure 7: Patterns in physical space (left) and Fourier space (right) when the initial condition is a scanned image of Figure (4). The pattern deteriorated over time.

waves described by the code originally propagated in a spatial direction, and the option of temporal evolution was given. Finally, the nonlinear time-dependent forcing term $c(t)$ in the GP equation had to be incorporated into the code [14]. The split-step method calls for an integration of ψ_N over what was time in my case. Now, the equation I integrated changed with time due to $c(t)$, so I had to add an extra loop.

6 Possible Future Work

After the SURF period was over, I was contacted by Professor Germán J. de Valcárcel regarding the initial conditions of the wavefunction. According to this information, $\psi(\mathbf{r}, 0) = \psi_{hom} + \text{perturbation}$, where the perturbation was a sum (over wavevectors) of waves with small random complex amplitudes [18]. For further work, the code could be tested using these initial conditions.

Before any further exploration is possible, it is necessary to affirm the validity of my split-step code. In the case of double-frequency forcing, superlattice patterns can appear if the forcing terms are separated by a phase shift, as has been found in the Faraday experiment [4]. In the Faraday case, patterns with 12-fold symmetry have been observed with a ratio of frequencies of 4:5 [16], triangular and hexagonal patterns appeared with a ratio of 1:2 [17], and 6:7 and 4:5 ratios have produced hexagonal patterns and superlattice patterns [17]. In the latter cases, if the amplitude of one of the forcing terms is much larger than the other, similar patterns are observed as if the weaker term were not present, and superlattice patterns only appear if the two forcing terms are of comparable magnitude [17]. A possible exploration is to use the GP equation to systematically explore how these observations hold in the case of BECs, and

how for BECs the superlattice patterns change as the ratios of the two forcing frequencies and amplitudes of modulation, and their phase shifts, are varied [4].

Using the transition curves as guidelines, one could plot the spatial atom density with parameters in stable and unstable regions, testing what happens for different values [10].

Acknowledgements

I would like to thank Mason Porter, my mentor, who provided invaluable guidance throughout this project. Also, his other SURF students, Kris Kazlowski, Tom Mainiero, Austin Webb, and Yan Zhang gave me helpful feedback. Tom Mainiero especially helped me figure out some features of Mathematica and scanned in an image, Figure 4, to convert it to a matrix. I would also like to thank my friend Oleg Rudenko for explaining some parts of differential equations to me. The code to solve partial differential equations by the split-step method was originally written by Martin Centurion. Professor Hermann Riecke gave me permission to take Figure 1 from his website [4]. Moreover, Professor Germán J. de Valcárcel provided me with the initial conditions for the wavefunction ψ , and gave me permission to use Figure 4, which appeared in his paper [5]. Finally, the SURF program and the Richter Memorial Funds funded this research opportunity.

References

- [1] Viñals, J., Faraday Waves. <http://www.physics.mcgill.ca/~vinals/research/fwaves/9> February 2006.
- [2] Lifshitz, R., Pattern Formation in Faraday Waves. Condensed Matter Physics. 1999. California Institute of Technology. 24 September 2006. <http://hades.caltech.edu/~lifshitz/patterns.html>
- [3] Cross, M. C. & Hohenberg, P. C., 1993. Pattern formation outside of equilibrium. *Reviews of Modern Physics* 65, (3), 851-1112.
- [4] Riecke, H. & Echebarria, B., 2001. Sideband Instabilities and Defects of Quasipatterns. *Physica D* 158, 1-4, 45-68.
- [5] Staliunas, K. & Longhi, S., & de Valcarcel, G. J., 2002. Faraday patterns in Bose-Einstein condensates. *Physical Review Letters* 89 (210406).
- [6] Kudrolli, A. & Gollub, J.P., 1996. Patterns and spatiotemporal chaos in parametrically forced surface waves: a systematic survey at large aspect ratio. *Physica D* 97, 133-154.

- [7] Silber, M., Topaz, C.T. & Skeldon, A.C., 2000. Two-frequency forced Faraday waves: weakly damped modes and pattern selection. *Physica D* 143, 205-225.
- [8] Ketterle, W., 1999. Experimental Studies of Bose-Einstein Condensation. *Physics Today* 52, 30-35.
- [9] Burnett, K. & Edwards, M., & Clark, C.W., 1999. The Theory of Bose-Einstein Condensation of Dilute Gases. *Physics Today* 52, 37-42.
- [10] Rand, R.H., 2005. Lecture Notes on Nonlinear Vibrations. <http://www.tam.cornell.edu/randdocs/nlvibe52.pdf>
- [11] Jordan, D.W. & Smith, P., 1987. *Nonlinear Ordinary Differential Equations*. Oxford University Press.
- [12] Nahfeh, A.H. & Mook, D.T., 1995. *Nonlinear Oscillations*. Wiley-IEEE.
- [13] Zounes, R.S. & Rand, R.H., 1998. Transition Curves for the Quasi-Periodic Mathieu Equation. *SIAM Journal of Applied Mathematics* 58, 4, 1094-1115.
- [14] Centurion, Martin. Propagation through a material with a positive n_2 and negative n_4 , MATLAB code, California Institute of Technology
- [15] Newell, A.C. & Moloney, J.V., 2003. *Nonlinear Optics*. Addison-Wesley Publishing Company, Redwood City, CA.
- [16] Edwards, W.S. & Fauve, S., 1993. Parametrically excited quasicrystalline surface waves. *Physical Review E* 47, 2, R788–R791.
- [17] Kudrolli, A. & Pier, B. & Gollub, J.P., 1998. Superlattice Patterns in Surface Waves. *Physica D* 123, 99-111
- [18] Valcárcel, G.J., private communication, 6 September 2006.